A study on the role of powertrain system dynamics on vehicle driveability

To appear in -
Vol. 00, No. 00, Month 20XX, 1–16

A Study on the Role of Powertrain System Dynamics on Vehicle Driveability

Luca Castellazzi[a]*, Andrea Tonoli[a], Nicola Amati[a] and Enrico Galliera[b]

[a] *Department of Mechanical and Aerospace Engineering, Mechatronics Laboratory, Politecnico di Torino, Corso Duca degli Abruzzi, 24, Turin, Italy*
[b] *C.R.F. S.C.p.A, Strada Torino 50, 10043 Orbassano, Italy*

(*v4.0 released October 2014*)

Vehicle driveability describes the complex interactions between the driver and the vehicle, mainly related to longitudinal vibrations. Today, a relevant part of the driveability process optimization is realized by means of track tests, which require a considerable effort due to the number of parameters (such as stiffness and damping components) affecting this behavior. The drawback of this approach is that it is carried on at a stage when a design iteration becomes very expensive in terms of time and cost. The objective of this work is to propose a light and accurate tool to represent the relevant quantities involved in the driveability analysis, and to understand which are the main vehicle parameters that influence the torsional vibrations transmitted to the driver. Particular attention is devoted to the role of the tire, the engine mount, the dual mass flywheel and their possible interactions. The presented non linear dynamic model has been validated in time and frequency domain and, through linearization of its non linear components, allows to exploit modal and energy analysis. Objective indexes regarding the driving comfort are additionally considered in order to evaluate possible driveability improvements related to the sensitivity of powertrain parameters.

Keywords: Driveability, Drivetrain Dynamics, Sensitivity Analysis, Transmission Design

1. Introduction

The term driveability describes the driver's complex subjective perception of the interactions between himself and the vehicle, associated to longitudinal acceleration aspects. Today, in the general context of Noise, Vibrations and Harshness (NVH), it has become a key factor for marketability and competitiveness of passenger cars.

Despite the availability of a number of simulation tools, even today driveability of passenger cars is still evaluated by means of a considerable amount of experimental tests on prototypes to measure important variables like longitudinal acceleration and jerk [1]. Subjective judgement still plays an important role, but the trend is to translate metrics as shuffles, kicks, jerks, hesitations, oscillations and overshoots into objective evaluation criteria based on measurements [2].

The result is that a good driveability rating is obtained after a long calibration process of the internal combustion engine (ICE) control algorithms, or by a fine tuning of each element of driveline components (e.g. flywheels, gearbox, half shafts) [3]. This is in contrast with the need of minimizing the tests on prototypes, reducing the *"time to market"*

*Corresponding author. Email: luca.castellazzi@polito.it

and the development costs.

Adequate mathematical models are therefore extremely useful at preliminary design stage to fix the main driveline component parameters. Similar models are useful also at later design stages, before prototype construction, for engine calibrations. The literature on the subject is summarized here below.

Couderc *et al.* [4] presented a work about the prediction of the dynamic behavior of vehicle drivelines including idle and drive gear rattle. They evidenced the need of having a nonlinear model especially for the study of the gear mesh, clearances and clutch friction effects. The lumped parameter model includes the torsional degrees of freedom of the whole driveline (flywheel, clutch assembly, gearbox, differential, half shafts, wheels and vehicle inertias) as well as the longitudinal degrees of freedom of vehicle chassis and engine block. Wheels are assumed to be connected to the ground, with negligible slip. Linearized equations allow a frequency domain analysis.

Farshidianfar *et al.* [5] underlined how drivelines are lightly damped non-linear systems possessing many degrees of freedom with strong coupling between the various subsystems. They can be excited by a large number of sources, affecting the vehicle NVH. They proposed a distributed parameters approach to model driveshafts and half shafts, while flywheel, clutch, gearbox, differential and wheels are modeled as lumped parameters. They demonstrated that this approach is able to identify the high frequency components associated with noise and vibration ("clonk").

Qatu *et al.* [6] analyzed the influence of the powertrain mount system at idle. The proper selection of both the support location and stiffness can improve the vehicle NVH behavior.

Capitani *et al.* [7] evidenced that the main driveability information have to be searched at about 10 Hz. They emphasized the presence of two main resonances in the longitudinal acceleration spectrum, the first at around 4 - 5 Hz (as function of the engaged gear) and the second at twice that value. A 9 DOF dynamic model is proposed, with the vehicle body modeled as an equivalent inertia. A simplified 2 DOF model including engine inertia and equivalent vehicle inertia connected by stiffness and damping can be used for control design purposes.

Hayat *et al.* [8] evidenced how vehicle driveability is a consequence of the optimization of many vehicle subsystems (e.g. suspensions, chassis, driveline). They proposed a model including the driveline and the vehicle body, showing a good numerical vs. experimental comparison. A model order reduction technique based on activity indexes is then applied to build a lighter and more effective macroscopic model including only relevant phenomena.

Sorniotti [9] analyzed driveline models with different level of complexity. The simplest includes just the compliance of the half shafts, an intermediate model takes into account the tire equivalent damping and the clutch damper, a detailed model considers the chassis dynamics too, including the suspensions and engine mounts. A deep sensitivity analysis has then been performed demonstrating that a significant coupling occurs between sprung/unsprung mass and the engine/gearbox/differential group.

Galvagno *et al.* [10] studied the so called 'Through the Road Parallel Hybrid Electric Vehicle' architecture from the driveability point of view. A 16 degrees of freedom, coupled torsional - longitudinal linear dynamic model is adopted to study the frequency response function between engine torque (input) and seat longitudinal acceleration (output), evidencing the presence of the first natural frequency of the transmission in the range of 1 - 10 Hz, depending on the gear ratio.

The actual trend of downsizing and supercharging the engines has the goal of reducing the fuel consumptions but leads to the drawback of increasing the vibrations. Consid-

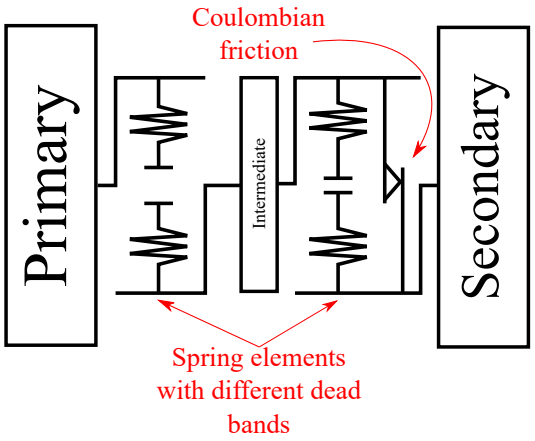

Figure 1. DMFW Schematic.

ering the relationship between injection parameters and the engine vibration level [11], sometimes adequate ignition strategies are implemented to reduce the torque irregularities. The main drawback is that they are not designed for engine efficiency optimization. Therefore, the need of vibrations attenuation systems plays an important role.

One powertrain element that has become popular in the last two decades is the Dual Mass Flywheel (DMFW). Figure 1 reports a schematic representation of the DMFW [12]. It is characterised by spring and damping elements connecting the primary and the secondary flywheels. Their assembly is thought to develop a nonlinear characteristic by means of parallel spring connections and proper dead bands. Coulombian friction is the main damping contribution to dissipate part of the vibrational energy. The intermediate flywheel is introduced only for constructional purposes. The main dead band is introduced to decouple engine vibrations from the rest of the driveline at idling. The second one to introduce a proper nonlinear effect of the stiffness. Spring stiffnesses are tuned soft enough to add the proper low frequency resonance.

The functionality of the DMFW regarding the attenuation of the torsional vibrations on the secondary flywheel connected to the primary shaft of the gearbox has been widely analyzed (i. e. [13], [14], [15]). Nevertheless the role played by the DMFW on driveability in terms of longitudinal acceleration of the seat rail against limit representative driving maneuvers has not been studied deeply yet.

The aim of the present work is to understand which are the main parameters influencing the filtering behavior of the transmission for what driveability is concerned. The frequency range of interest includes oscillations up to 30 Hz, characteristic of ride and shake vibratory phenomena and therefore correlated to human comfort [16]. Higher order effects such as those relative to gear rattle and whine involve higher frequency contributions and are therefore neglected.

The comprehension of which powertrain parameters are able to improve the vehicle driveability brings direct information that can be translated into design objectives.

A complete vehicle dynamic model is proposed to this end, including DMFW, engine mounts, longitudinal compliances of the unsprung masses and tire. The model is validated both in time and frequency domain. The linearization of its nonlinear components (e. g. DMFW, clutch and tire), allows performing modal and energy analysis in addition to sensitivity analysis.

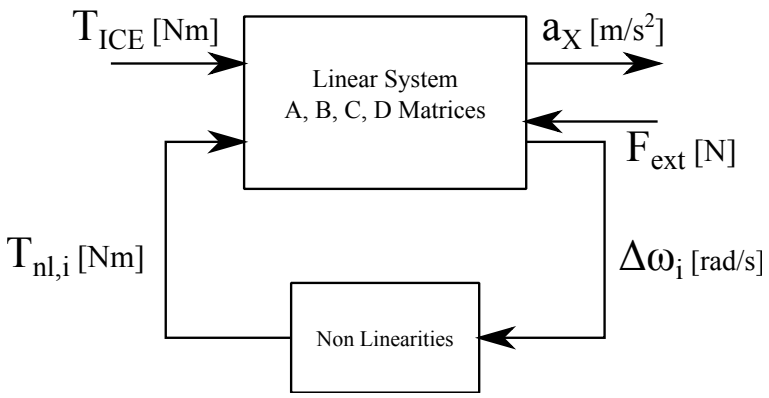

Figure 2. General block diagram schematization of the model.

2. Vehicle Dynamics Model

Figure 2 shows the general block diagram representation of the model. The main inputs to the system are the torque coming from the ICE (T_{ice}) depurated from the belt drive losses and the generalized external forces F_{ext}, that take aerodynamic, grade and rolling resistances into account. The linear system block includes all linear contributions to the model (written in state space form in terms of its state, input and output matrices A, B, C, D). The nonlinear effects are included by a feedback block that takes the angular speed differences across the nonlinear elements $\Delta\omega_i$ to determine the corresponding nonlinear torques $T_{\text{nl},i}$. Making reference to Fig. 3 the vehicle model is now described in detail.

Driveline. Engine inertia and primary DMFW inertia are merged together in one flywheel (J_1). Clutch cover is merged with the secondary inertia of the DMFW (J_2). k_1 is the DMFW nonlinear spring while damper c_1 models the viscous losses in parallel to it. The Coulombian friction is modeled with a hyperbolic tangent function:

$$T_{\text{DMFW,fric}} = C \cdot tanh\left(\frac{\Delta\omega}{\omega_{\text{ref},1}}\right) \tag{1}$$

where $\Delta\omega$ is the relative angular speed between flywheels J_1 and J_2. C and $\omega_{\text{ref},1}$ have been identified from the experimentally measured hysteresis cycles of the DMFW characteristic.

Clutch torque T_{c} is modeled as a bilinear function of the relative angular speed ($\Delta\omega$) between J_2 and J_{d} (clutch disc inertia), modulated by the axial load F of the clutch actuation systems:

$$T_{\text{c}} = nfFr_{\text{m}} \cdot f\left(\Delta\omega\right) \tag{2}$$

where $f\left(\Delta\omega\right)$ is a slip function described as

$$f\left(\Delta\omega\right) = \begin{cases} c_{\text{c}1}\Delta\omega & \text{if } |\Delta\omega| < \Delta\omega_0 \\ c_{\text{c}2} & \text{if } |\Delta\omega| \geq \Delta\omega_0 \end{cases} \tag{3}$$

n is the number of surfaces in contact, f is the friction coefficient between the friction

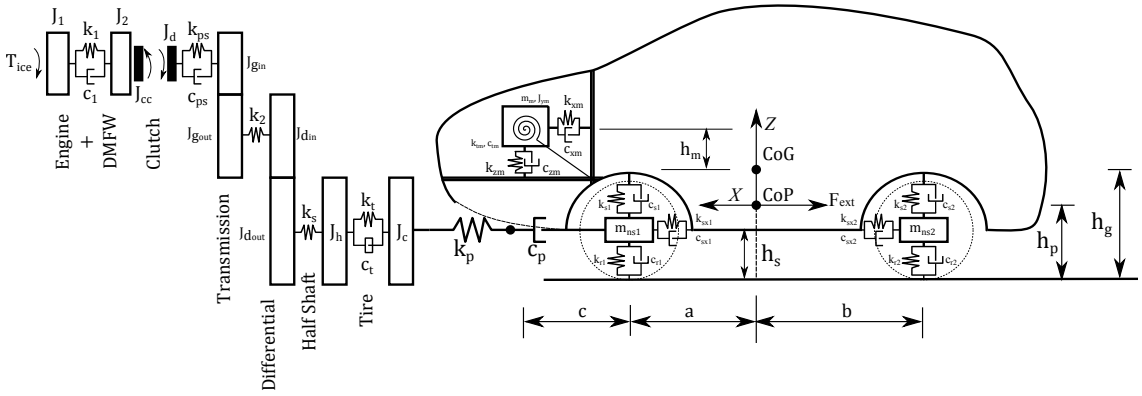

Figure 3. Coupled torsional - longitudinal dynamic model.

surfaces, r_m is the mean value of the disc radius, $\Delta\omega_0$ is a reference speed value and c_{c1} and c_{c2} are experimentally measured slip values. Clutch pedal position is translated into the actual axial load F by means of an experimental curve that characterizes the clutch actuation system. It is implemented in the model non linearities (Fig.2).

Clutch characteristics are modeled with the nonlinear spring k_{ps} and viscous damper c_{ps}. A standard 6 gears manual transmission is considered with the active stage of reduction (2 flywheels, J_{gin} and J_{gout}) according to the engaged gear. Final reduction is modeled as fixed transmission ratio with associated inertias J_{din} and J_{dout}. k_2 models the transmission shaft.

The half shafts are modeled as springs with stiffness k_s. They connect the carrier of the differential to the wheel hub. Hub and tire belt inertias (J_h and J_c) are connected to the torsional stiffness and damping of the belt itself (k_t and c_t). The *Tire* contact forces couple the torsional and longitudinal dynamic behavior. As described in [17] they are modeled as the series connection of a spring and a viscous damper to take slip and relaxation length into account. This behavior can be described by a first order differential equation in terms of the longitudinal contact force F_x as a function of the unsprung mass speed V_{us} and tire belt speed $\omega_c R$:

$$\frac{dF_x}{dt} + \frac{k_p}{c_p} F_x = V_{us} - \omega_c R \tag{4}$$

where k_p is the tire longitudinal stiffness and c_p is the longitudinal slip coefficient. The expressions for k_p and c_p are the following:

$$k_p = \frac{b_w \cdot F_z}{a_w}; \qquad c_p = \frac{b_w \cdot F_z}{V_x} \tag{5}$$

where b_w is the slope of the $\mu_x - \sigma$ curve of the tire (longitudinal adherence vs longitudinal slip), F_z is the vertical load including the effect of the load transfer due to longitudinal accelerations, a_w is half length of the contact patch and V_x is the longitudinal vehicle speed.

Chassis and Suspensions. Vertical suspension characteristics are modeled as a parallel connection of springs and dampers (k_{s1}, k_{s2} and c_{s1}, c_{s2}), connected to the sprung (m_s) and the unsprung masses (m_{ns1} and m_{ns2}). Sprung mass rotates in its pitch motion

around the pitch centre (CoP). Longitudinal suspension characteristics are taken into account by linear spring and damper elements (k_{sx1}, k_{sx2} and c_{sx1}, c_{sx2}). They take into account the longitudinal compliance of the elastomeric bushings of the suspension arms and the bushings of the subframe.

Finally k_{r1}, k_{r2} and c_{r1}, c_{r2} represent the vertical stiffnesses and dampings of the tire. The road is considered dry and flat with no vertical irregularities.

The *Engine* and transmission case is modeled as a rigid body with mass and polar moment of inertia (m_{m}, J_{ym}), connected to the sprung mass by means of *engine mounts* with linear longitudinal, vertical and torsional stiffness and damping characteristics (k_{xm}, k_{zm}, k_{tm} and c_{xm}, c_{zm}, c_{tm}). Yaw and roll engine mounts properties are neglected due to the absence of such generated motions in the model [18].

Synchronizers are not included in the model because incorrect engagement maneuvers are not taken into account. For a given gear, the linear portion of the system is represented in state space in terms of its A, B, C, D matrices. The change between two different gears is simulated by changing these matrices according to the appropriate transmission ratio.

Nonlinear characteristics such as that of the DMFW are implemented as look up tables. In alternative they are linearized with their local slope corresponding to a given torque level. Similarly, the tire characteristics are linearized considering a given vertical load and vehicle speed V_{x}.

3. Time and Frequency Domain Simulations and Validation

The aim of time and frequency domain validations is to understand if the model is robust enough to reproduce the desired phenomena in the relevant frequency range for driveability analysis (up to about 30 Hz). To this end, experimental longitudinal accelerations are acquired by means of AVL Data Acquisition System using a 3 - axis accelerometer ASC 5521 with 0 - 5 V analog input sampled with 100 Hz of frequency. The accelerometer is rigidly fixed to the seat rail. Tests are conducted on a dry road. The torque input to the model is the one coming from the estimation of the engine control unit. In most of the maneuvers this estimation has an accuracy that is higher than 95 %. In some maneuvers this accuracy could not be guaranteed.

Experimental acceleration is compared with the one predicted by the model. Two numerical results are obtained. The first one, called linearized, is obtained linearizing the DMFW and clutch stiffness characteristics with their local slopes. Constant values are given to the vertical load F_{z} and the vehicle speed V_{x} to linearize the tire. The second one, called 'nonlinear', takes into account all the nonlinear components of the powertrain.

Figure 4a shows a comparison between numerical and experimental vehicle longitudinal acceleration during a tip in - tip out maneuver in 2nd gear. The nonlinear model shows a good fit both in the tip in and in the tip out phases. A much less damped response of the linearized model is justified by the fact that most of the dissipation in the system is due to the dry friction in the DMFW and clutch. These dissipations are taken into account in the nonlinear model but have not been considered in the linear one, as well as those due to the tire.

Longitudinal acceleration during an upshift maneuver is plotted in Fig. 4b, showing a good correlation also during these phases. The engaged gear is shown in the figure but the corresponding gear ratios are not included for confidentiality reasons.

Numerical and experimental longitudinal accelerations during a full load maneuver in 2nd gear engaged are compared in Fig. 4c showing a good correlation. Rather strong oscillations can be evidenced, especially during motoring phases of the engine (about 45

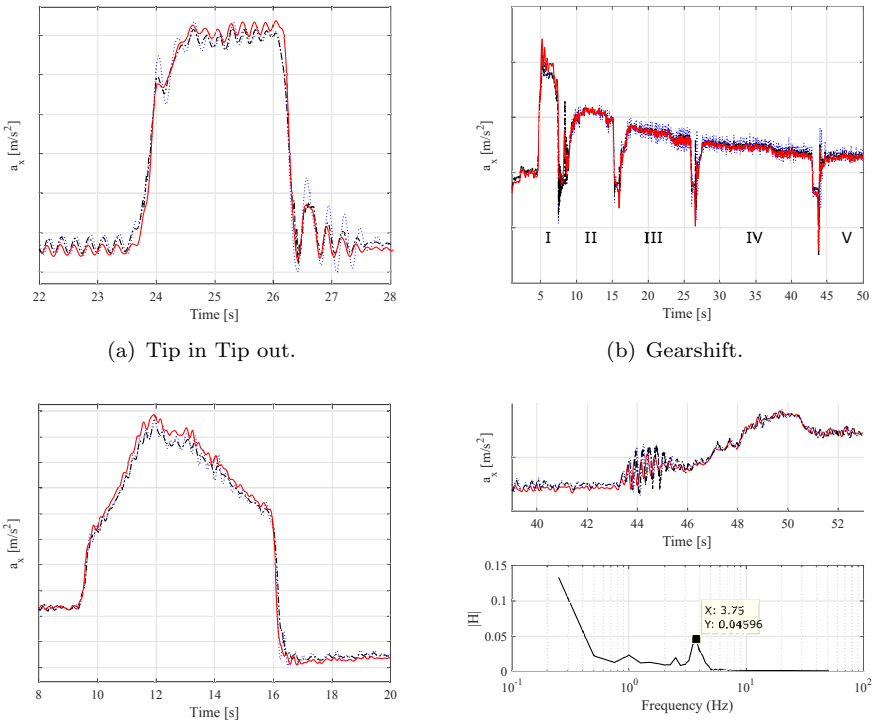

(a) Tip in Tip out.

(b) Gearshift.

(c) Motoring and Full Load.

(d) Motoring and Full Load (different time frame).

Figure 4. Vehicle longitudinal acceleration, comparison between numerical and experimental results (dotted blue: numerical linear model, dashed dotted black: numerical nonlinear model, continuous red: experimental). y - axis ticks are omitted for confidentiality reasons.

seconds of the simulation, Fig. 4d) with a frequency of about 3 - 4 Hz. As it will be seen later, they are ascribed to the oscillations of, among other components, the DMFW, that in these engine conditions plays a fundamental role in the filtering behavior of the transmission system. The nonlinear model is actually slightly less damped with respect to the experimental data; this can be due to the difficulty to find reliable data about lubricants effects in the various components of the driveline. The small discrepancy between numerical and experimental signals at steady state could be ascribed to a less precise estimation of the engine torque by the engine control unit during the release phases (closed throttle, negative engine torque). The phase shift between the two numerical results is ascribed to different DMFW stiffness properties included in the linear and nonlinear model.

Time domain comparisons are useful as a first step of the model validation process, because they allow to understand if the degree of detail of the model is enough to reproduce the experimental signals. A second step of the model validation process is performed in frequency domain.

Time domain data during a tip in - tip out experiments/simulations have been used to compute the frequency response function between the engine torque (input) and the vehicle longitudinal acceleration (output). Such maneuver is considered suitable for this purposes because of its ability to ideally excite all the system modes. The response is compared in Fig. 5 to that obtained from the linearized model. The comparison shows a good match up to about 10 Hz. For higher frequencies the input and output experimental signals are affected by a low coherence due to the 100 Hz sampling rate.

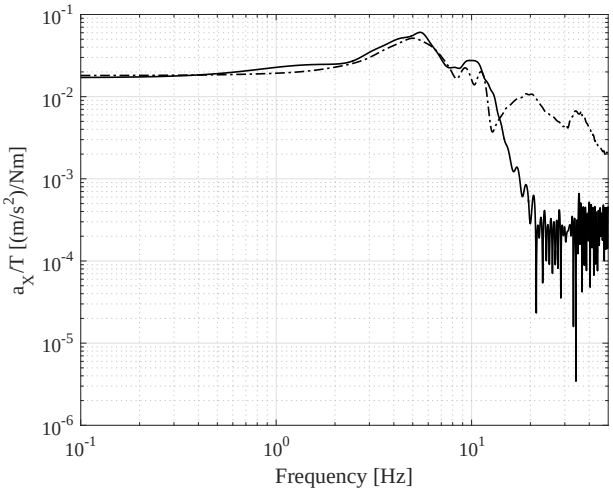

Figure 5. Comparison between numerical (dashed dotted line) and experimental (continuous line) frequency response functions.

4. Sensitivity Analysis on Powertrain Parameters

One of the most interesting characteristic of a powertrain system is the *engine to driver* dynamic behavior. This refers to its ability to filter out the mechanical vibrations that are generated inside the ICE in order to obtain a smooth and non oscillatory behavior of the longitudinal acceleration that otherwise could affect the drive quality.

Modal analysis is performed on the linearized model to determine the natural frequencies of the system. Then, modal energy is computed to investigate the sensitivity of the system to the design parameters. These are mostly related to the stiffness of the filtering components (DMFW, engine suspensions).

4.1. *Modal and Energy Analysis*

The natural frequencies of the system have been computed as eigenvalues of the linearized system state matrix (Fig. 2).

Modal energy analysis has then been performed to understand the contribution of each spring to the modal potential energy. To this end, for each mode of vibration j, the modal energy contribution U_{ij} has been computed as the ratio between the energy stored in the generic spring i, and the total energy stored at each mode for all the springs:

$$U_{ij} = \frac{\frac{1}{2}k_i \left(\psi_{i,j} - \psi_{i+1,j}\right)^2}{\frac{1}{2}\{\psi\}_j^T [K] \{\psi\}_j} \tag{6}$$

where matrix [K] is the stiffness matrix of the linearized system and $\{\psi\}_j$ is the eigenvector associated to the j-th mode.

Figure 6 shows a color map representation of the modal energy contribution U_{ij} of the 15 model stiffnesses on the first 11 modes. Four main *mode clusters* are evidenced with the letters A, B, C and D. Cluster A is dominated by the chassis modes in terms of vertical shaking and pitch motion, as evidenced by the amount of energy stored in suspension springs k_{s1} and k_{s2}. Cluster B is dominated by the DMFW (spring k_1), the half shafts

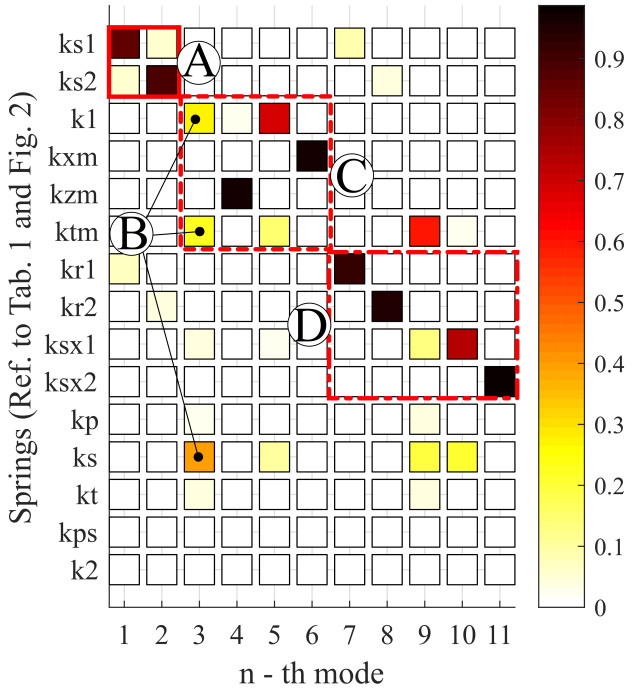

Figure 6. Modal energy contribution of the different springs in modes 1 to 11, corresponding to a frequency range between 1 and 35 Hz. 2nd gear engaged.

(spring k_s) and the torsional engine mount (spring k_{tm}). Cluster C is dominated mainly by the engine mount dynamics in terms of longitudinal, vertical and torsional motion of the powertrain with respect to the chassis body. Cluster D is dominated by vertical and longitudinal motions of the unsprung masses (front and rear). It is worth to note the coupling effects that are clear evident in some clusters, less in others. It should be taken into account that these couplings are subjected to modifications if different gears are engaged. Table 1 explains more in detail the different modes of vibrations in terms of involved degrees of freedom.

Modes between 3rd and 6th are relative to the 3 - 15 Hz range (Tab. 1) and belong to clusters B and C. This is a very important interval of frequencies for vehicle driveability and comfort purposes because the most severe engine harmonics are attenuated in this range. A fundamental role is played by the DMFW and the engine suspension as they act exactly in this frequency range.

The role of the different modes is also evidenced in the frequency response function between input torque and output longitudinal acceleration of the undamped system (Fig. 7). The 4 clusters are evidenced with the same figures used in Fig. 6. A *low pass filter* trend is shown and the cut off frequency is dominated by the first powertrain natural frequency (B cluster).

Figure 8a shows the same frequency response function including the effect of the damping as function of the different speeds of the vehicle. Increasing the speed, the curves show a more damped behavior. This effect is caused by the tire ground contact model (Eq. 4). For low speeds, damping is so high that its role in dissipating energy is negligible. Increasing the speed, tire contact damping c_p decreases, so its deformation increases with the effect of dissipating more energy and reducing the amplitude of the resonance peaks.

Figure 8b shows the effect of the engaged gear on the same transfer function for con-

Table 1. Natural frequencies, associated components and modes of vibration (refer to Fig. 6). Legend: L = Longitudinal, V = Vertical, T = Torsional, P = Pitch, Y = Yes, N = No.

Mode	Frequency [Hz]	Associated component	Mode of Vibration	Gear Influence (%)
1	1.1	Body	V, P	N
2	1.3	Body	V, P	N
3	4	DMFW, half shafts, engine block	T	Y (100%)
4	8.5	Engine block	V	N
5	9.7	DMFW, engine block, half shafts	T	Y (22%)
6	11	Engine block	L	Y (18%)
7	13	Front unsprung mass	V	N
8	17	Rear unsprung mass	V	Y (6%)
9	18	Engine block, front unsprung mass, half shafts	T, L	Y (5%)
10	25	Front unsprung mass, half shafts	T, L	Y (8%)
11	32	Rear unsprung mass	L	N

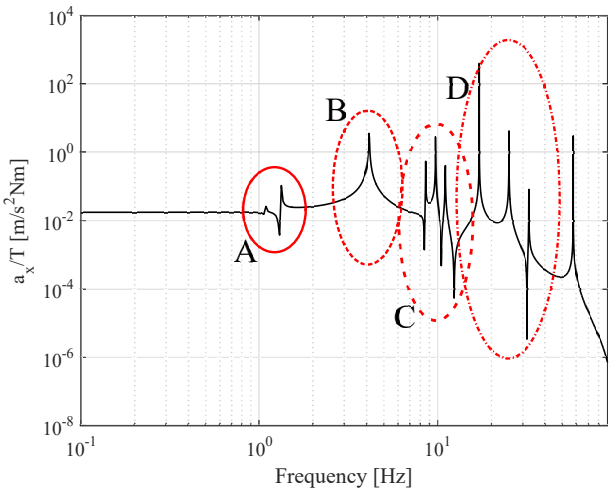

Figure 7. Frequency response function between input torque and vehicle longitudinal acceleration of the undamped system. 2nd gear engaged.

stant speed. For low frequencies the response is dominated by the equivalent overall inertia:

$$G = \left.\frac{a_{\mathrm{x}}(\omega)}{T_{\mathrm{in}}(\omega)}\right|_{\omega=0} = \frac{i_{\mathrm{g}} \cdot i_{\mathrm{d}}}{R \cdot m_{\mathrm{e}}} \tag{7}$$

where i_{g} and i_{d} are the transmission ratios of the gearbox and of the differential respectively, R is the effective rolling radius of the tire and m_{e} is the apparent (or equivalent) mass of the vehicle taking the translating masses and the rotating inertias into account.

Additionally, it is noticeable that the engaged gear affects the cut off frequency of the DMFW moving it to higher frequencies if higher gears are engaged. Above the cut off frequency the response is little affected. The influences of the engaged gear on the aforementioned frequency response function and modal potential energy are also present in [19].

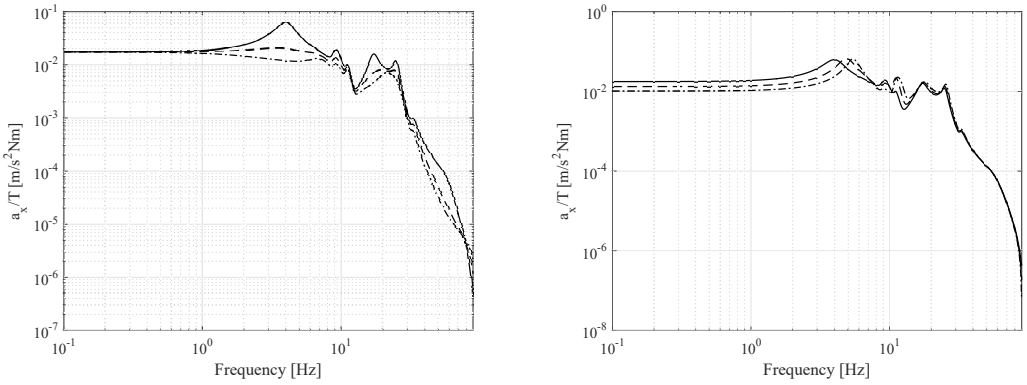

Figure 8. Frequency response function between input torque and vehicle longitudinal acceleration of the damped system in 2nd gear as function of the different vehicle speed (a) (continuous line: $V = 20$ km/h, dashed line: $V = 70$ km/h, dashed dotted line: $V = 120$ km/h). Frequency response function between input torque and vehicle longitudinal acceleration of the damped system at constant speed ($V = 20$ km/h) as a function of the different engaged gear (b) (continuous line: 2nd gear, dashed line: 3rd gear, dashed dotted line: 4th gear).

4.2. *Sensitivity Analysis*

A standard powertrain system can be analyzed from its two basic functions. The first is to realize the proper transmission between the internal combustion engine and the wheels, matching vehicle loads and engine torque. The second, less obvious, is to attenuate the vibrations coming from the engine.

The previous study has evidenced the central role played by the DMFW and the engine suspension in the filtering behavior of the powertrain. This motivates the investigation of the sensitivity of the resonant frequencies as a function of the DMFW and torsional engine mount stiffness. A strong influence is expected in the mid frequency range (B, C cluster in Fig. 7, 3 - 15 Hz) due to what evidenced in the modal energy analysis.

To this end, stiffness k_1 and k_{tm} have been varied between -80% to +100% of their nominal value.

Half shafts have actually an influence in the same range of frequencies and their role has been evidenced. Sensitivity on this powertrain component will not be performed because already present in literature [9].

Figure 9 shows the first 6 natural frequencies in 2nd gear as a function of the individual variation of DMFW stiffness (k_1, continuous black) and torsional engine mount stiffness (k_{tm}, dashed red). Being the first two modes relative to bounce and pitch motion of the sprung mass, their natural frequencies remain constant in all the parameters range. By converse, as already evidenced in Fig. 6, the third mode is strongly affected, among others, by the DMFW stiffness. It is interesting to note that this mode is also affected by the torsional engine mount stiffness, which produces a variation of the natural frequency comparable to that due to the DMFW stiffness.

Cluster C is comprehensive of modes related to the engine block. Therefore, fourth, fifth and sixth modes are coupled modes. Considering DMFW stiffness variation, it is shown that fourth mode is influenced only for variations lower than - 30%. Conversely, sixth mode is insensible to variations smaller than + 40%. In the middle, fifth mode increases its natural frequency only for DMFW stiffness variations in between the above-mentioned percentages. The three natural frequencies never cross each other and a veering phenomenon occurs.

Torsional engine mount stiffness variation does not generate veering (apart in the nonrealistic case of -70 % of reduction). Fifth mode increases its frequency with stiffness increase, fourth and sixth modes are almost not sensible.

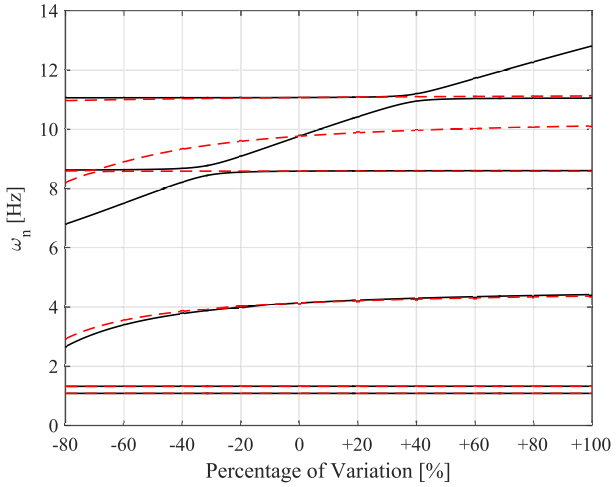

Figure 9. First 6 natural frequencies of the system as a function of the variation of the DMFW stiffness (continuous black) and of the torsional stiffness of the engine mounts (dashed red). 2nd gear engaged.

Figure 10 shows the frequency response function between input torque and output longitudinal acceleration when DMFW and engine mount torsional stiffnesses are varied together. Nominal, half and twice of their values have been considered while the other parameters are the same as for Fig. 9 (20 km/h, 2nd gear engaged).

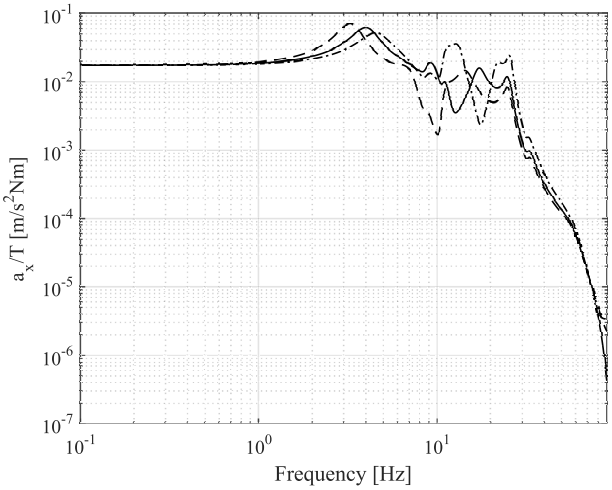

Figure 10. Frequency response function between input torque and vehicle longitudinal acceleration in 2nd gear engaged considering a sensitivity on both the DMFW stiffness k_1 and the torsional engine mount stiffness k_{tm}. Continuous line: nominal values, dashed line: half of the nominal values, dashed dotted line: twice the nominal values.

The main effect of the DMFW and engine mount stiffness variation is in the frequency range of clusters B and C (3 - 15 Hz). Reducing the stiffnesses lowers the first powertrain frequency and improves the attenuation in the same range of frequencies. Increasing the

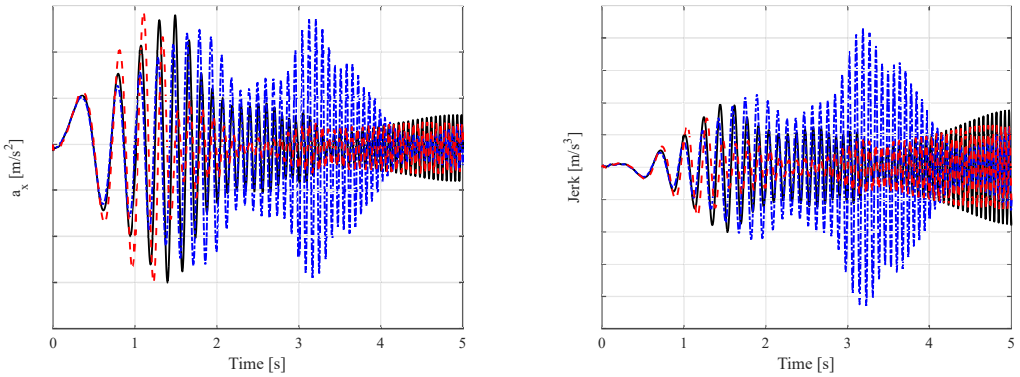

(a) Longitudinal acceleration (b) Jerk

Figure 11. Longitudinal acceleration (a) and jerk (b) for sine sweep maneuver in 2nd gear engaged considering a sensitivity on both the DMFW stiffness k_1 and the torsional engine mount stiffness k_{tm}. Continuous line: nominal values, dashed line: half of the nominal values, dashed dotted line: twice the nominal values.

stiffnesses above the nominal values reduces the attenuation in the same band and leads to larger amplitudes of the cluster C modes.

Additionally, doubling DMFW and torsional engine mount stiffnesses, two peaks of the frequency response function are present between 6 and 15 Hz. This confirms that the DMFW and the torsional engine mount modes intimately interact with each other similarly to a dynamic vibration absorber.

High frequency modes (more than 30 Hz) do not show any variation, consistently with the fact that the passive powertrain components are effective only in a limited frequency range.

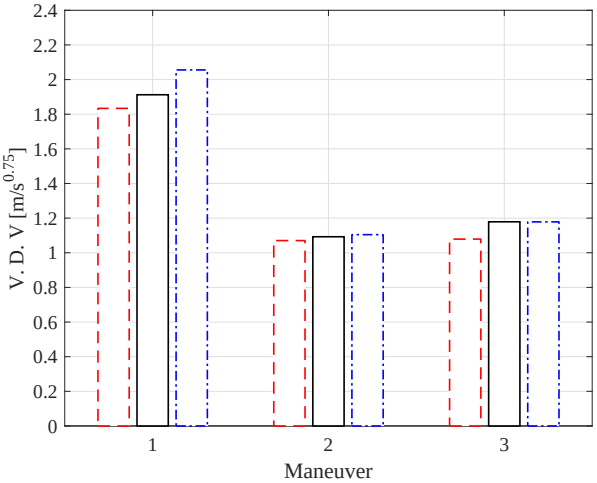

Figure 12. Vibration Dose Value computed for the three considered maneuvers (1: sine sweep, 2: Tip In - Tip Out, 3: Full Load) for the case of nominal stiffness values (continuous), half of the nominal stiffness values (dashed) and twice the nominal stiffness values (dashed dotted).

DMFW and torsional engine mount stiffness modifications are also evaluated in time domain by fully nonlinear simulations performed with same input torque and same parametric variations of DMFW and torsional engine mount stiffness.

A first analysis has been performed with a sine sweep torque input with frequency variation from 0.1 to 20 Hz in 5 seconds to have a simple correlation with the frequency response function of Fig. 10. The longitudinal acceleration and jerk of Fig. 11 show that the smaller the DMFW and torsional engine mount stiffness, the higher the vibration attenuation. The large amplitudes between 1 and 2 seconds are due to the excitation of modes between 3 and 7 Hz. Increasing the stiffness from half (dashed line) to twice (dashed dotted line) the nominal value, the first peak of accelerations occurs at slightly later times but with a second burst appearing between 3 and 4 seconds. The same burst is even more evident in the jerk. This is in agreement with the frequency response function of Fig. 10.

The same time domain analysis have then been repeated with giving the experimental tip in - tip out and full load engine torque as input to the nonlinear model. For the sake of brevity, the responses are not shown but the benefits of different DMFW and engine mount setups can be evaluated by computing the Vibration Dose Value (VDV), a measure of the total vibration experienced by the human driver in contact with vibrating surface [20]. It can be used as an objective parameter for the evaluation of the driving comfort. VDV is expressed as:

$$VDV = \int_{t_0}^{t_f} \tilde{a}^4(t)dt \tag{8}$$

where $\tilde{a}$ is a frequency weighted acceleration using a bandpass filter between 1 and 32 Hz [21]. t_0 and t_f are starting and final simulation time.

Fig. 12 shows the computed VDV for the three different maneuvers described before (1: sine sweep, 2: Tip In - Tip Out, 3: Full Load) for the three stiffnesses variations (dashed bars: half, continuous bars: nominal, dashed dotted bars: twice).

The reduction of the DMFW and torsional engine mount stiffness with respect to its nominal value reduces the VDV for all of the three maneuvers; conversely, their increment increase the VDV. Sine sweep maneuver (1) seems to be the most sensitive regarding the variation of vibration dose value with respect to the parameters variation. This can be related to the large amplitude of the 10 - 15 Hz modes in case of stiffnesses increment.

Full load maneuver (3) shows a lower influence of the VDV with respect to the stiffnesses variation. The lower are the stiffnesses, the lower is the VDV even though the variation is quite small (about 10% with respect to the largest value in the same maneuver).

Furthermore, Tip in - Tip (2) out shows the lowest VDV sensitivity with respect to the stiffnesses variation for all the considered maneuvers. Small value of VDV is anyway found considering stiffnesses reduction.

Finally, the analysis suggests the need of a stiffnesses tradeoff in order to obtain a good balance between filtering performance and avoidance of excessive deflections during maximum torque transmission or starting phases.

5. Conclusions

The paper describes a dynamic model for vehicle driveability analysis. The model has been validated by extensive time domain validations with different maneuvers, showing a good correlation between numerical and experimental results. Analysis in the frequency domain completed such comparison. The model has been structured in order to split the

linear and nonlinear components in order to highlight the role played by the nonlinear contributions meanwhile exploiting modal and energy analysis. The effect of the different powertrain component parameters on the system natural frequencies has been evidenced in addition to their role played on the transmissibility of the engine torque to the vehicle longitudinal acceleration. The coupling between the DMFW and engine mount stiffness is a new result that can drive future design choices. Their combined low pass filter action is underlined. The results are confirmed by time domain analysis based on standard reference maneuvers and computing the vibration dose value comfort index. Concluding, the key role of tire, engine suspension and dual mass flywheel is then explained. Tire affects the vibrations transmissibility as a function of the vehicle speed and the engine suspension, together with the dual mass flywheel, dominate the mid - range dynamics and govern the transmissibility function of the powertrain.

References

[1] Choi YC, Song HB, Lee JH, Cho HS. An Experimental Study for Drivability Improvements in Vehicle Acceleration Mode. Proceedings of the Institution of Mechanical Engineers, Part D: Journal of Automobile Engineering, Vol. 217, No. 7, 2003.

[2] List HO, Schoeggl P. Objective Evaluation of Vehicle Driveability. SAE Tehcnical Paper 980204, 1998.

[3] Dorey RE, Holmes CB. Vehicle Driveability - Its Characterization and Measurement. SAE Technical Paper, 1999 - 01 - 0949, 2001.

[4] Couderc P, Callenaere J, Der Hagopian J, Ferraris G, Kassai A, Borjesson Y, Verdillon L, Gaimard S. Vehicle Driveline Dynamic Behaviour: Experimentation and Simulation. Journal of Sound and Vibration, Vol. 218, No. sv981808, 1998.

[5] Farshidianfar A, Ebrahimi M, Bartlett H. Hybrid Modelling and Simulation of the Torsional Vibration of Vehicle Driveline Systems. Proceedings of the Institution of Mechanical Engineers, Part D: Journal of Automobile Engineering, Vol 215, No. 215, 2001.

[6] Qatu M, Sirafi M, Johns F. Robustness of Powertrain Mount System for Noise, Vibration and Harshness at Idle. Proceedings of the Institution of Mechanical Engineers, Part D: Journal of Automobile Engineering, Vol. 216, No. 805, 2002.

[7] Capitani R, Delogu M, Pilo L. Analysis of the influence of a vehicle's driveline dynamic behavior regarding the performance perception at low frequencies. SAE Technical Paper 2001 - 01 - 3333, 2001.

[8] Hayat O, Lebrun M, Domingues E. Powertrain Driveability Evaluation: Analysis and Simplification of Dynamic Models. SAE Technical Paper, 2003-01-1328, 2003.

[9] Sorniotti A. Driveline Modeling, Experimental Validation and Evaluation of the Influence of the Different Parameters on the Overall System Dynamics. SAE Technical Paper, 2008-01-0632, 2008.

[10] Galvagno E, Morina A, Sorniotti A, Velardocchia M. Drivability analysis of through-the-road-parallel hybrid vehicles. MECCANICA. vol. 48 n. 2, pp 351-366. - ISSN 0025-6455.

[11] Carlucci A P,.Chiara F F, Laforgia D. Analysis of the relation between injection parameter variation and block vibration of an internal combustion diesel engine. Journal of sound and vibration 295.1 (2006): 141-164.

[12] Cariccia G, Giansetto G, Montani A, Guala A. Dual Mass Flywheel. U. S. Patent 0338493, 2014.

[13] Schaper U, Sawodny O, Mahl T, Blessing U. Modeling and torque estimation of an automotive Dual Mass Flywheel. 2009 American Control Conference. IEEE, 2009.

[14] Mahl T, Sawodny O. Modelling of an automotive dual mass flywheel. IFAC Proceedings Volumes 43.18 (2010): 517-523.

[15] Galvagno E, Velardocchia M, Vigliani A, Tota A. Experimental Analysis and Model Validation of a Dual Mass Flywheel for Passenger Cars. SAE Technical Paper 2015-01-1121, 2015, doi:10.4271/2015-01-1121.

[16] Morello L, Rosti Rossini L, Pia G, Tonoli A. The Automotive Body, Vol. II: System Design, MES, pp. 239 - 363.

[17] Pacejka H, Besselink I. Tire and Vehicle Dynamics. Third Edition, Elsevier, ISBN: 978-0-08-097016-5, 2012.

[18] Genta G, Morello L. The Automotive Chassis, Volume 2: System Design. Springer, 2009.
[19] Castellazzi L, Tonoli A, Amati N, Piu A, Galliera E. Vehicle Driveability: Dynamic Analysis of Powertrain System Components. SAE Technical Paper 2016-01-1124, 2016.
[20] Jauch C, Bovee K, Tamilarasan S, Guvenc L, Rizzoni G. Modeling of the OSU EcoCar 2 vehicle for Drivability Analysis. IFAC - PapersOnLine 48 - 15 (2015) 300 - 305.
[21] Horste K. Objective Measurement of Automatic Transmission Shift Feel Using Vibration Dose Value. SAE Technical Paper, 951373, 1995.